Synthesis and Characterization of Ion-Exchangeable Titanate Nanotubes

Xiaoming Sun and Yadong Li*[a]

Abstract: Titanate nanotubes were synthesized under hydrothermal conditions. The optimized synthesis (100–180 °C, longer than 48 h), thermal and hydrothermal stability, ion exchangeability and consequent magnetic and optical properties of the titanate nanotubes were systematically studied in this paper. First, nanotubes with monodisperse pore-size distribution were prepared. The formation mechanism of the titanate nanotubes was also studied. Second, the thermal and hydrothermal stability were characterized with X-ray diffraction (XRD), high-resolution transmission electron microscopy (HRTEM), Fourier transform infrared (FTIR), and Raman spectroscopy. Results showed that sodium ions played a significant role in the stability of the frameworks. Third, the selective ion exchangeability was demonstrated with a series of ions. The ion substitution also enlarged the BET surface area of the titanate nanotubes to 240 $m^2 g^{-1}$. Combination of these two features implied that these nanotubes might be functionalized by substitution of different transitional-metal ions and consequently used for selective catalysis. Magnetism, photoluminescence, and UV/Vis spectra of the substituted titanate nanotubes revealed that the magnetic and optical properties of the nanotubes were modifiable.

Keywords: ion exchange · nanotubes · titanates · transition metals

Introduction

Mesoporous molecular sieves (silica[1] or non-silica[2]) with well-defined pore diameters of 2–50 nm (e.g. hexagonally ordered MCM-41), high surface area, and tunable pore size have shown great potential as versatile catalysts and catalysts supports. However, the relatively low thermal stability of the mesoporous materials limits their applications, since the properties of these materials such as catalytic durability and shape selectivity are ultimately dependent on the thermal and hydrothermal stability of these materials.[1b, 2, 3]

Crystalline nanotubes with uniform diameters and nanoporous structures would be ideal substitutes for such materials. Carbon nanotubes (CNT) have been extensively studied since their discovery in 1991,[4] and considering their molecular size and unusual mechanical and electrical properties, are considered the base of future electronics.[5] The large-scale synthesis[6] and functionalization of these tubular structures by doping, decoration, and encapsulation to expand their application field have been explored over the last few years. Nevertheless, both theoretical and experimental results show that their properties significantly depend on their diameter, thickness, helicity, and defect concentration.[5a, 7] The uncontrollability of helicity and the high synthetic cost, especially for high-purity samples, greatly limit the utilization of CNTs. At the same time, their hydrophobicity limits their applications in biochemistry, aqueous chemistry, and catalysis.[8]

A rational idea inspired by CNTs is that since graphite sheets can roll up into tubes, other inorganic materials with similarly layered structures might also function in this way. It is reasonable since the layers, held together mainly by weak van der Waals' forces, would lower the energy gap and rigidity by adopting a tubular morphology. Quite a few non-carbon nanotubes such as $B_xC_yN_z$,[9] MS_2 (M = Mo, W, Nb, Ta, etc.),[10] $NiCl_2$,[11] vanadium oxide,[12] InS,[13] and Bi[14] have been synthesized under favorable conditions. Theoretical studies also confirmed this point of view.[15]

Unlike the layered compounds mentioned above, many important metal oxides such as TiO_2, MnO_2, ZrO_2, Nb_2O_5 do not exhibit layered structures, since the strong ionic interactions keep the metal cations and oxygen anions together. Nanotubes from these nonlayer-structure materials generally require templates (e.g. carbon nanotube[16] or anodic alumina oxide[17]) to give spatial confinement, with the walls generally amorphous or semicrystalline. However, TiO_2 nanotubes were claimed by several groups as counter examples, where no layered structures existed.[18] Since titanium is widely used because of its catalytic activity, whether in the form of TiO_2[19]or as photo-excitable moieties in zeolite frameworks,[20] the titania nanotubes attracted wide attention as soon as it was discovered. Si-substituted nanotubes were also reported and the catalytic properties were characterized.[21]

[a] Prof. Y. Li, X. Sun
Department of Chemistry, Tsinghau University
Beijing 100084 (P.R. China)
Fax: (+86) 10-62788765
E-mail: ydli@tsinghau.edu.cn

 DOI: 10.1002/chem.200204394

However, doubts exist concerning the formation and construction of these nanotubes. In the reports,[18, 21] the so-called titania nanotubes were obtained by alkaline hydrothermal treatment of titania or mixtures of TiO_2/SiO_2, followed by washing with water and a 0.1M HCl aqueous solution. TEM observations indicated the existence of layered structures, but no reported phase of titania had layered structures similar to the titanates and hydrous titanates.[22] Selected-area electron diffraction (SAED) patterns were presented as evidence to demonstrate that the crystal structure of the nanotubes could be indexed to anatase.[18a] It was not possible to repeat this,[23] and elemental analysis indicated a variety of atomic ratios of Ti/O. Furthermore, XRD, a general strategy to characterize crystal structural features, was not used in the original study. Some results reported on the so-called TiO_2 nanotubes were hard to understand. For instance, the amount of water existing in products was 20 times larger than that of the starting materials, and $H_2Ti_3O_7 \cdot 0.5\,H_2O$ could dehydrate to TiO_2 (B) in a water washing process, with former dehydration processes realized at temperature as high as 500 °C.[21a]

The doubts were first raised by us about two years ago,[24] following experimental evidence presented by Peng et al.[23] In this paper, the structural stability, ion exchangeability and consequent properties of titanate nanotubes were systematically studied. First, we optimized the synthetic procedure, and a direct hydrothermal hydrolysis from anatase TiO_2 to large quantities of pure multiwall crystal titanate nanotubes (with almost uniform inner diameters of 5 nm, outer diameters of 10 nm and lengths of about 300 nm), was realized at 100 °C–180 °C in 5–10M NaOH solution. In this process we found that dispersion in alcohol affected the morphology and agglomeration of the final products. Monodisperse nanotubes were obtained by using the improved method. Second, energy-dispersive X-ray analysis (EDXA) of the different tubular samples demonstrated the presence of sodium ions, and the determination of the thermal stability revealed the stabilization effect of sodium ions on the tubular framework structure. The frameworks were maintained even after thermal treatment at 550 °C for 5–10 h. Third, ion exchangeability and hydrothermal stability of the nanotubes were demonstrated by hydrothermal substitution of transition-metal ions such as Co^{2+}, Ni^{2+}, Cu^{2+}, Zn^{2+}, Cd^{2+}, and Ag^{+}. The substituted nanotubes were well characterized with powder X-ray diffraction (XRD), transmission electron microscopy (TEM), selected-area electron diffraction (SAED), and EDXA. Magnetism measurements, photoluminescence, and UV/Vis spectra of the substituted titanate nanotubes revealed that the magnetic and optical properties of the nanotubes were modifiable by introducing different transition-metal ions.

Experimental Section

Synthesis of titanate nanotubes: The method employed for the synthesis of titanate nanotubes was essentially the same as described in reference [1b]. All chemicals used in this work were A.R. reagents from the Beijing Chemical Factory, except where otherwise indicated. In a typical synthesis, titania powder (0.5 g, about 5 nm in size, prepared by using a published method[26]) and an aqueous solution of NaOH (10M, 40 ml) were placed into a Teflon-lined autoclave. The mixture was stirred to form a milklike suspension, sealed and hydrothermally treated at 100–180 °C for more than two days. The precipitate was separated by filtration and washed with deionized water until a pH value near 8 was reached. The precipitate was then ground in alcohol followed by ultrasonic-assisted dispersion. After a second filtration and alcohol washing step, the sample was oven-dried at 80 °C for more than 4 h.

By optimizing the concentration of NaOH and the time of hydrothermal treatment, pure nanotubes could be produced by using different particle size (from several nanometers to several hundreds of micrometers) of the starting anatase TiO_2 powder.

Determination of the thermal and hydrothermal stability: The determination of the thermal stability of the products was carried out in a conventional tube furnace. The as-prepared titanate nanotubes were placed in a quartz boat, which was placed in the hot zone inside the quartz tube and heated to 550 °C in 2 h at a constant rate. The temperature was kept constant for periods from 20 min to 10 h before cooled to room temperature. All the heating processes were carried out in air.

The hydrothermal stability was determined in a Teflon-lined autoclave. The titanate nanotubes and deionized water was put directly into the autoclave and pH value was adjusted by adding HCl or ammonia solution. The autoclave was then sealed and hydrothermally treated at 100 °C for 5–10 h.

Ion-exchange reaction: Ion-exchange reactions were carried out in aqueous ammonia solution with Cd^{2+}, Zn^{2+}, Co^{2+}, Ni^{2+}, Cu^{2+}, and Ag^{+} respectively, because of the stability of titanate nanotubes in basic solution and the stabilization of these substituting ions by complexation with ammonia. In a typical process, excess amount of salts of the corresponding ions were dissolved in water followed by adding analytical ammonia solution drop by drop to form clear solutions. The titanate nanotubes were then dispersed in the respective solutions and stirred for 10–20 h or irradiated in an ultrasonic generator for 100 min for sufficient dispersion and diffusion. Products were carefully washed with dilute ammonia and deionized water several times to avoid physical adsorption of the substituting ions on the surface of the titanate nanotubes.

Characterization of samples: Powder XRD was performed on a Bruker D8 Advance X-ray diffractometer with monochromatized $Cu_{K\alpha}$ radiation ($\lambda =$ 1.5418 Å). The size and morphology of titanate nanotubes were measured by using a Hitachi H-800 transmission electron microscope (200 kV). The layered structure of the nanotubes was revealed by high-resolution transmission electron microscopy (HRTEM, JEOL JEM-2010F transmission electron microscope, 200 kV). Raman (Renishaw RM1000 Raman spectrometer, excitation wavelength 514 nm) and Fourier transform infrared spectra (Perkin-Elmer Spectrum GX) were used to characterize the structure of samples. The chemical compositions of the samples were determined with EDXA, X-ray photoelectron spectroscopy (PHI 5500ESCA system, $Al_{K\alpha}$ X-ray source), and thermogravimetric analysis (TGA)/differential thermogravimetry (DGT) (TA instruments, TGA2050). A Mettler-Toledo DSC821e differential scanning calorimeter (DSC) was used to examine phase behavior of samples at a constant heating rate of 10 °C min^{-1}. The temperature-dependent molar magnetic-susceptibility data for Co-substituted nanotubes were obtained in the temperature range 4–300 K at 5000 G on a SQUID magnetometer. The optical properties of samples were characterized by photoluminescence (Perkin Elmer LS50B Luminescence Spectrometer operated at room temperature) and UV/Vis diffuse-reflectance spectroscopy (Shimadzu UV-2100S spectrophotometer).

Results and Discussion

The quality of these synthesized titanate nanotubes was of great significance for the determination of the ion-exchangeability and thermal stability. We carefully studied the synthesis process, and confirmed the point of view of Kasuga et al. that the washing process was the key to obtaining the tubular structure.[18b]

In earlier reports on titanate nanotubes, the washing process merely involved washing with water. In our case, acetone and alcohol were used to disperse the white precipitate, taken from the NaOH solution, directly without washing with water, and typical TEM images are shown in Figure 1a and Figure 1b, respectively. Samples dispersed in alcohol yielded mainly monodisperse nanotubes, while samples dispersed in acetone afforded mainly vesicles. These vesicles shrank under irradiation with an electron beam, and were finally changed to aggregate-like depositions. A few nanotubes were found with the vesicles, but these might exist due to residual water. This result implied that alcohol was a good dispersant and aided the formation of titanate nanotubes. Alternatively, if we washed the white precipitate with water, followed by dispersion in acetone or alcohol, nanotubes of similar morphology were found in both cases. These results demonstrated that the nanotubes were formed in the washing and dispersing process, and once formed, remain stable.

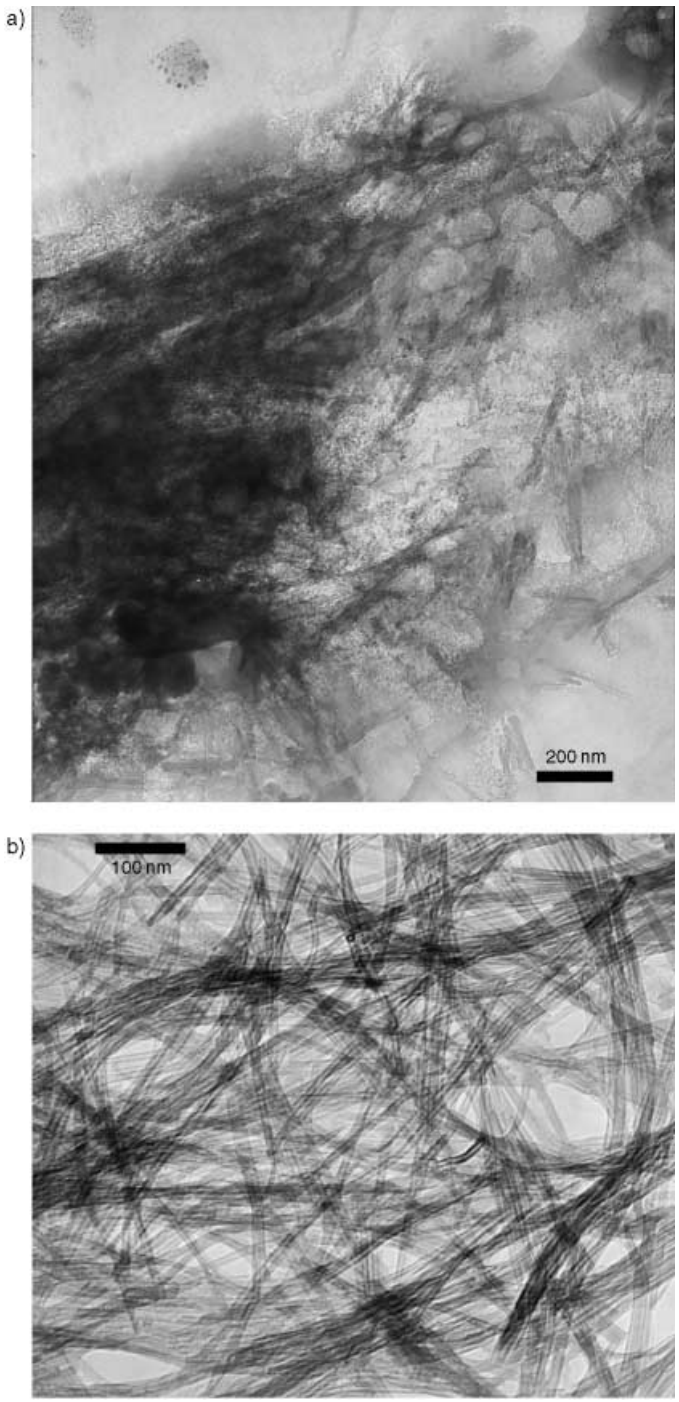

Figure 1. TEM images of the crude white precipitation taken from the 10 M NaOH solution and dispersed in a) acetone, and b) alcohol. In the latter image, monodispersed nanotubes are shown clearly.

We also demonstrated that the use of alcohol enabled the formation of aggregation-free nanotubes. This was evidenced by the pore-size distribution obtained from the Barrett–Joyner–Halenda (BJH) deposition curve, which showed that the merely water-washed nanotubes exhibit two peaks (Figure 2a). The peak positioned at 3.7 nm is considered to correspond to the inner diameter of nanotubes, while the other broad peak positioned in the range of 8 to 20 nm is probably caused by the aggregation of nanotubes. However, when these nanotubes were ground in alcohol, then dispersed in a large amount of alcohol by using ultrasonic irradiation, and subsequently oven-dried, the nanotubes exhibited a pore-size distribution centered at 3.7 nm, with no other peaks in the range from 2 to 100 nm (Figure 2b). The pore-size distribution, unlike the TEM observations, was obtained from the statistical information of a large number of nanotubes, thus the disappearance of the second peak in Figure 2b implied the separation of most nanotubes from one another.

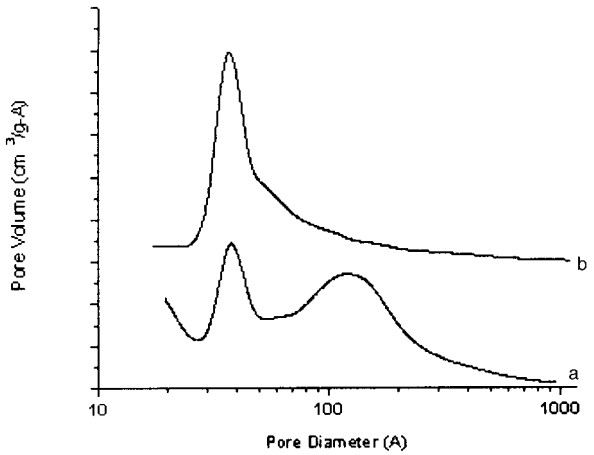

Figure 2. The pore-size distribution obtained from the BJH deposition curve of titanate nanotubes obtained for samples a) washed with water, and b) dispersed with alcohol following the washing with water.

We also compared the sample obtained by washing with water only and that obtained after subsequent washing with acid. Results showed that the residual sodium ions in the titanate nanotubes played an important role. It was difficult to remove the sodium completely, even after the sample had been washed for three days and when the final pH value of the suspension of titanate nanotubes reduced from 11 to 8. As dilute acid was added to adjust the pH value to 7, some sheets were observed (Figure 3). It was found that when a sample was washed with dilute acid, the sodium ions were substituted by protons and consequently reduced the static electronic interactions between the titanate sheets.

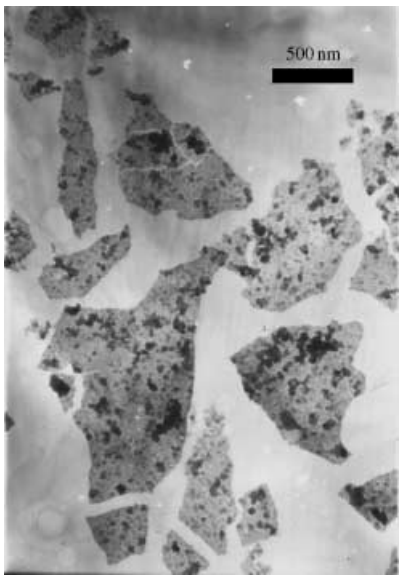

Figure 3. The sheets formed in the suspension of titanate nanotubes as dilute acid was added to adjust the pH value of the suspension to 7.

The resulting changes were revealed by TGA and XRD studies. The TGA plots corresponding to different washing times and consequently different final pH values, 8 (Figure 4a) and 11 (Figure 4b), indicated that a lower pH value resulted in a greater weight loss. This is reasonable since more protons replace sodium ions at lower pH, which then evaporated at high temperature.

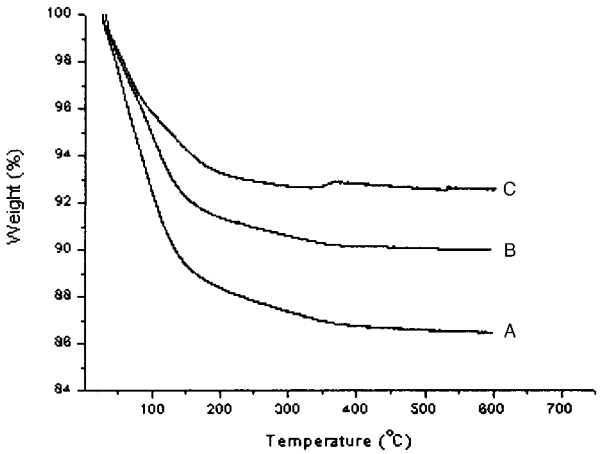

Figure 4. TGA plots of different titanate nanotubes, a) titanate nanotubes washed with water until pH = 11, oven-dried; b) titanate nanotubes washed with water until pH = 8, oven-dried; c) titanate nanotubes heated at 550 °C for 1 h and then exposed to air for 1 h.

The XRD pattern of nanotubes obtained after washing with water only (Figure 5a) could be indexed to $H_2Ti_3O_7$ according to current structural investigations.[26] We prefer to consider it as a kind of titanate nanotube that might be described as $Na_xH_{2-x}Ti_3O_7$ ($x \approx 0.75$) according to our EDXA studies and the determination of the thermal and hydrothermal stability.

The nanotubes obtained revealed quite good thermal stability, which was illustrated by comparison between the XRD patterns of the crude titanate nanotubes (Figure 5a) and

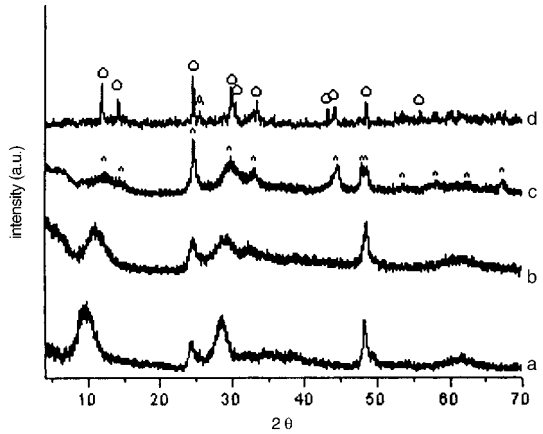

Figure 5. XRD patterns of the titanate nanotubes and their derivatives after calcination at different temperatures: a) the crude titanate nanotubes synthesized by hydrothermal methods at 140 °C for two days; b) the titanate nanotubes after calcination at 550 °C (the pattern is very similar to that in a), indicating the maintenance of crystal structure); c) the sodium titanate nanotubes calcinated at 600 °C, which could be indexed to $Na_2Ti_9O_{19}$ (marked with ′′), indicating the degradation of nanotube structure; d) the sodium titanate nanotubes calcinated at 850 °C, in which a mixture of $Na_2Ti_6O_{13}$ and anatase TiO_2 was observed and marked with ′O′($Na_2Ti_6O_{13}$) and ′A′(anatase), respectively.

those of the samples after calcination at 550 °C (Figure 5b) for 5 h. The essentially identical patterns indicated the maintenance of the crystal structure of the titanate framework, without degradation, at 550 °C. However, when the nanotubes were calcined at 600 °C for 20 min, a new phase of titanate, $Na_2Ti_9O_{19}$ formed (Figure 5c), which was consistent with the atomic ratio of Na/Ti of $Na_xH_{2-x}Ti_3O_7$ ($x \approx 0.75$) given above. When the nanotubes were calcined to 850 °C, $Na_2Ti_9O_{19}$ transformed to a mixture of $Na_2Ti_6O_{13}$ and TiO_2 (Figure 5d).

Washing with acid also had a notable effect on the thermal stability. In the XRD patterns of titanate nanotubes obtained after stirring in 0.1 M nitric acid for 2 h (Figure 6b), reflections at 10° and 28° were significantly weakened, indicating structural change. When the sample obtained after washing

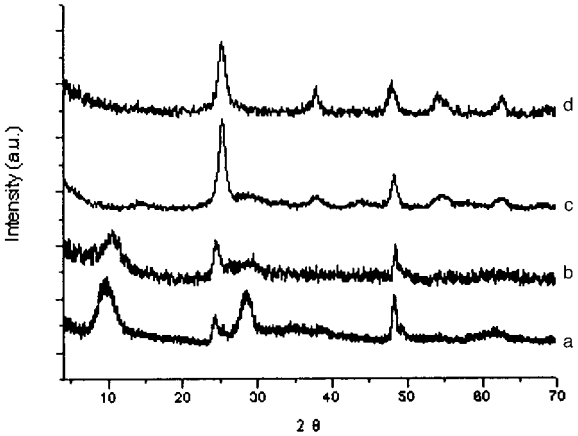

Figure 6. XRD patterns of starting titanate nanotubes and acid-washed samples: a) XRD pattern of starting titanate nanotubes; b) XRD pattern of titanate nanotubes after stirring in 0.1 M HNO_3 for 2 h; c) XRD pattern of titanate nanotubes after thermal treatment at 500 °C for 1 h following stirring in 0.1 M HNO_3 for 2 h; d) XRD pattern of titanate nanotubes after hydrothermal treatment in 0.1 M HNO_3 at 100 °C for 7 h, which have transformed completely to anatase.

with acid was thermally treated at 500 °C for only 1 h, the sample was completely transformed to titania (anatase phase) according to its XRD pattern (Figure 6c). This implied that the thermal stability of nanotubes was strongly dependent on the presence of sodium ions, which was highly surprising.

The determination of the hydrothermal stability further demonstrated the important role of sodium ions. When a sample was hydrothermally treated in dilute nitric acid (pH 2) at 100 °C for 7 h, titania powder (anatase) was formed, as evidenced by the XRD reflections (Figure 6d). The framework of the tubular structure was still retained in ammonia solution, even after hydrothermal treatment in ammonia solution (5 mol L^{-1}) at 120 °C for 10 h (according to the characterization by XRD and the subsequent TEM image).

The thermal stability is of great significance for nanoporous materials,[3] and the results mentioned above indicate that the phase conversation took place in the temperature range between 550 and 600 °C. Here, the conversion temperature was found to be 565 °C according to an endothermic peak (marked with an arrow) in the DSC plot (Figure 7). The first endothermic peak in Figure 7 was attributed to dehydration of the sample.

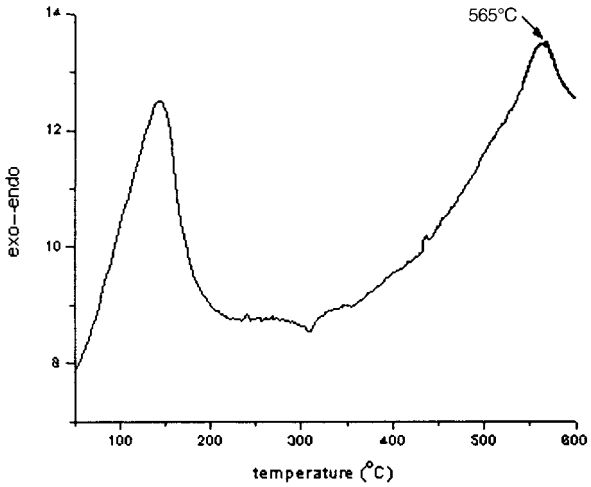

Figure 7. The DSC plot of the titanate nanotubes.

The morphological evolution under thermal treatment was also studied by TEM. High-resolution TEM images (Figure 8a) indicated that the starting nanotubes were multilayered nanotubes with an interlayer distance of 0.8 nm. Notably, this value is smaller than the value of 0.9 nm calculated from the reflection at $2\theta = 10^\circ$ in the XRD patterns of the starting nanotubes (Figure 5a), but is consistent with the value obtained after dehydration at 550 °C (Figure 5b), for which the diffraction maximum had moved to $2\theta = 11^\circ$ ($d =$ 0.8 nm). The selected-area electron diffraction (SAED) patterns (inset in Figure 8a) recorded on an individual nanotube showed reflections characteristic of a tubular structure. Two spots at the edge of the zero spot were consistent with the layered structure of nanotubes. Diffraction spots are elongated in the direction perpendicular to the tube axis.

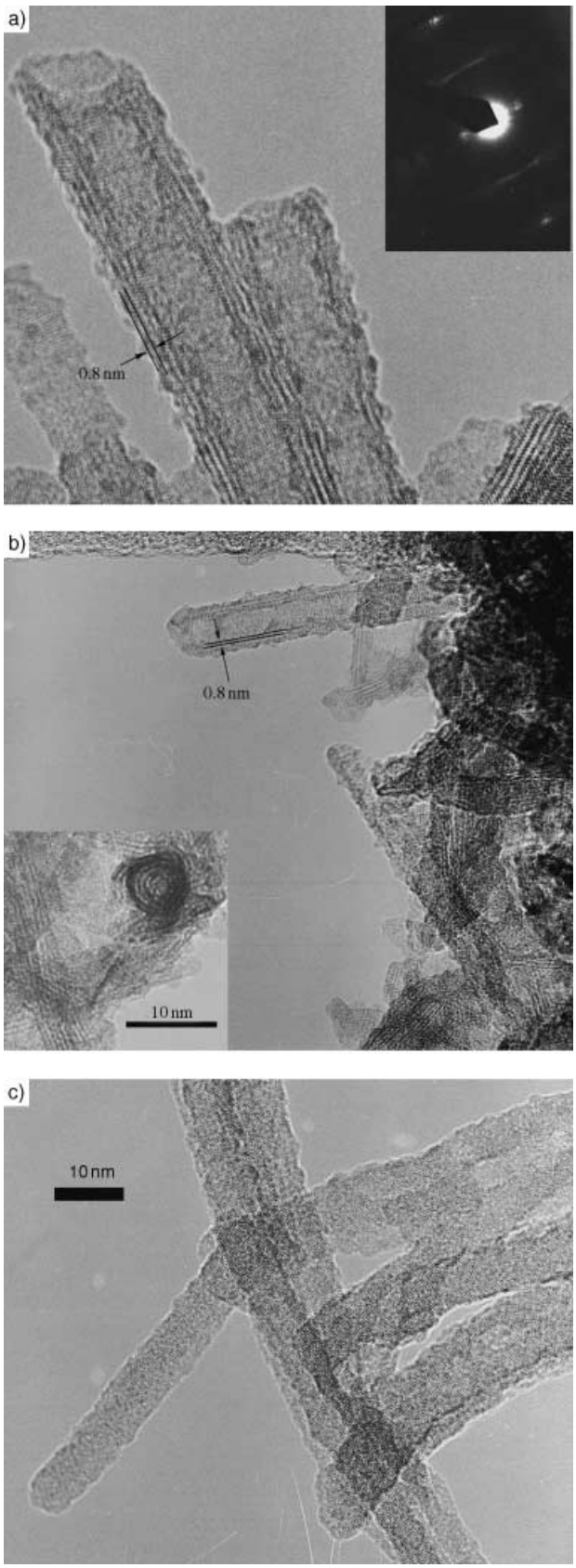

Figure 8. HRTEM images of titanate nanotubes before and after thermal treatment: a) A HRTEM image of starting titanate nanotubes, inset shows the SAED patterns recorded on an individual nanotube; b) HRTEM image of sample thermally treated at 550 °C, inset shows a cross-section view of an individual nanotube; c) HRTEM images of a sample thermally treated at 600 °C, where $Na_2Ti_9O_{19}$ nanowires were formed.

The reduction in the *d* value might be explained by the dehydration of the sample caused by focusing the electron beam on the sample under high vacuum, which is comparable to heating the sample to 550 °C. The HRTEM image (Figure 8 b) of a 550 °C thermally treated sample confirmed our proposal, where the found *d* value was also 0.8 nm. The cross-section view of an individual tube was recorded (the inset in Figure 8 b) with which both the tubular structure and the interlayer distance of 0.8 nm were further confirmed. A HRTEM image of a sample obtained after thermal treatment at 600 °C for 20 min (Figure 8 c) clearly showed the formation of fibrous $Na_2Ti_9O_{19}$ and the disappearance of the tubular structure.

The structural evolution under thermal treatment was also characterized by Raman spectroscopy. The Raman spectrum of titanate nanotubes (Figure 9 a) obtained after hydrothermal treatment and washing with alcohol was essentially the

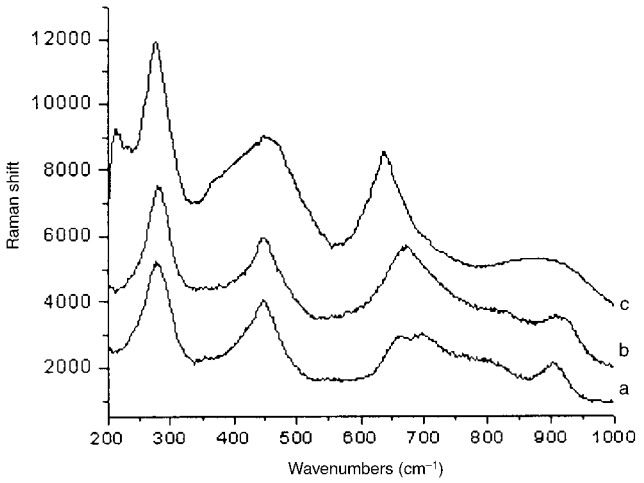

Figure 9. Raman spectra of samples before and after thermal treatment: a) sample obtained after water washing without heating; b) sample after thermal treatment at 550 °C for 1 h; c) sample after thermal treatment at 600 °C for 1 h.

same as that reported by Kasuga et al.,[18b] and similar to the spectrum of water-treated $Cs_2Ti_2O_5$.[27] The peak at about 905cm^{-1} was attributed to a four-coordinate Ti–O stretching vibration involving nonbridging oxygen atoms that are coordinated with Na ions .[28] The peak at 280 cm^{-1} was reported for a $Na_2O \cdot 2TiO_2$ glass.[29] After thermal treatment at 550 °C (Figure 9 b), no obvious difference was found since phase transformation did not take place. In Figure 9 c, which was recorded on a sample thermally treated at 600 °C, emergence of a peak at about 213 cm^{-1} and the shift of the peaks near 680 cm^{-1} to lower wavenumber indicated the formation of a new phase. The similarity of these three curves is a reflection of the similarity of the framework and coordination states of the local structures of the sodium titanates.

EDXA (Figure 10) studies performed on individual nanotubes exhibited the existence of Na and Ti with a molar ratio close to 1:4. This was consistent with $Na_2Ti_9O_{19}$, when the sample was heated to 600 °C, in which the ratio of Na to Ti was also near to 1:4. This result implied that the molar ratio of Na

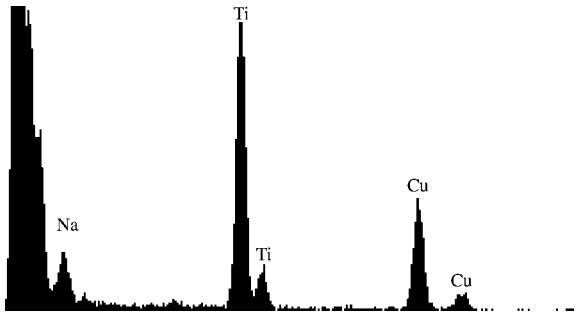

Figure 10. EDXA spectrum recorded on individual nanotubes, which exhibits the presence of Na and Ti with a molar ratio close to 1:4 (19.8:80.2).

and Ti of 1:4 might be favorable for the formation and maintenance of titanate nanotubes.

FTIR was also used to characterize the titanate nanotubes, and demonstrated the existence of large amounts of water and hydroxy groups because of the existence of a binding vibration of H-O-H at 1630 cm^{-1}, and a strong stretching vibration of O–H at 3400 cm^{-1}.[18b] Notably, nanotubes oven-dried at 100 °C for 4 h (Figure 11 a) or thermally treated at

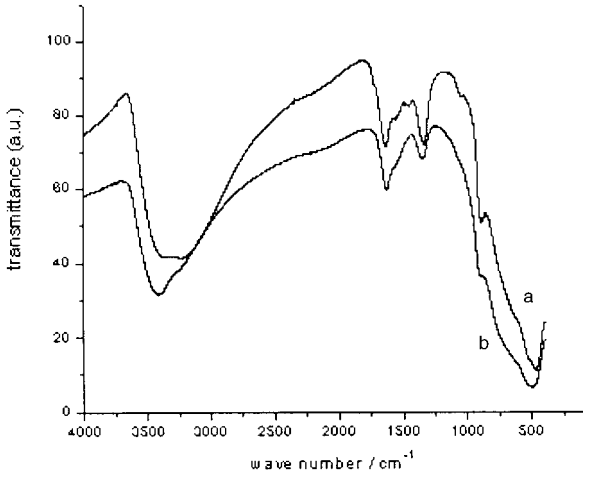

Figure 11. FTIR spectra of different titanate nanotubes: a) titanate nanotubes oven-dried at 80 °C for 4 h and then exposed to air for 1 h; b) titanate nanotubes thermally treated at 550 °C, and then exposed to air for 1 h.

550 °C for 20 min (Figure 11 b) exhibited essentially the same IR spectra after being exposed to air for more than 1 h. Both IR spectra were similar to that of previously reported acid-exchanged products of titanates.[21d] The existence of water and hydroxy groups in the sample after thermal treatment at 550 °C was attributed to re-adsorption of water from the atmosphere. The amount of adsorbed water in the thermally treated samples was quantified by TGA (Figure 4 c). The total weight loss of about 8 % for the sample thermally treated at 550 °C was attributed to dehydration of reabsorbed water. The hydroxylating tendency of titanate is similar to that of titania,[30] which provides a possibility to construct a humidity-sensitive detector[31] through a combination of this property and the semiconductivity of the titanate.

The introduction of transition metals or noble metals into the porous structures of nanoporous materials has been

extensively explored and demonstrated to be effective for promoting the selectivity and activity of the materials.[32] In the case of titanate nanotubes, ion exchange was shown to be achieved by simply stirring the nanotubes in solutions of the corresponding cationic ions. The large specific surface area and strong hydrophilic tendency might further facilitate the ion-exchange process.

As the nanotubes were stirred in the aqueous ammonium solutions of the ions under investigation, these transition-metal ions replaced the sodium ions. It should be noted that, at the same time, proton ions might also be substituted, and ammonia ions might also take part in the substitution. Their presence was proved by our experimental results.

XRD reflections of the transition-metal-ion-substituted nanotubes (Figure 12) were essentially the same as the starting material, implying the maintenance of the framework

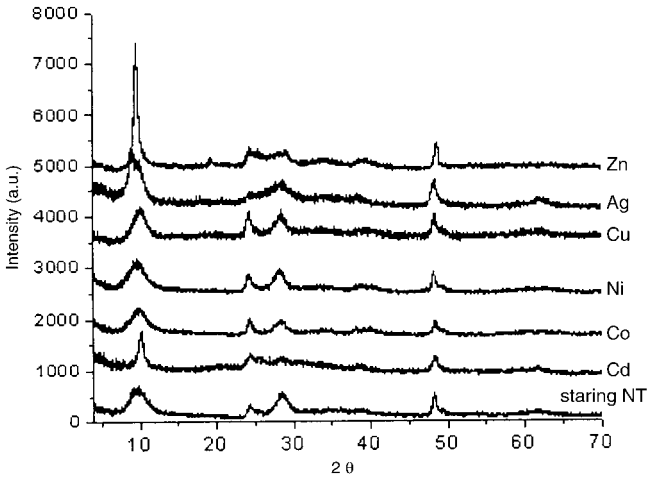

Figure 12. XRD patterns of the transition-metal-substituted titanate nanotubes (corresponding substituting metals are labeled; the pattern of the starting titanate nanotubes (NT) is shown for comparison).

and random distribution of substituted ions. TEM images revealed that the tubular structure was retained without the agglomeration of particles or clusters that are formed at the outer wall of nanotubes substituted with Co^{2+}, Ni^{2+}, Cu^{2+}, Zn^{2+}, Cd^{2+}, implying the homogeneously substitution of ions. TEM images of Co- and Ni-substituted derivatives are shown in Figure 13a and Figure 13b as examples. Corresponding EDXA plots shown in the insets indicated the existence of substituted ions and the absence of sodium ions. HRTEM images of Ni-substituted nanotubes (Figure 13c) gave further insight into the structure of substituted nanotubes, with no particles observed on the inner and outer surface of the nanotubes, and the layered structures still clearly visible.

The substitution of transition metals was further characterized by XRD and XPS. When the Co-substituted titanate nanotubes were heated to 850 °C for 1 h, this resulted in the formation of a mixture of $CoTiO_3$ and TiO_2 without the presence of sodium titanate (Figure 14), while the original starting titanate nanotubes transformed to give $Na_2Ti_9O_{19}$ or a mixture of $Na_2Ti_6O_{13}$ and TiO_2 at temperatures above 600 °C (Figure 5, curve d). The XPS spectra also supported the conclusions from the XRD results that the substitution was

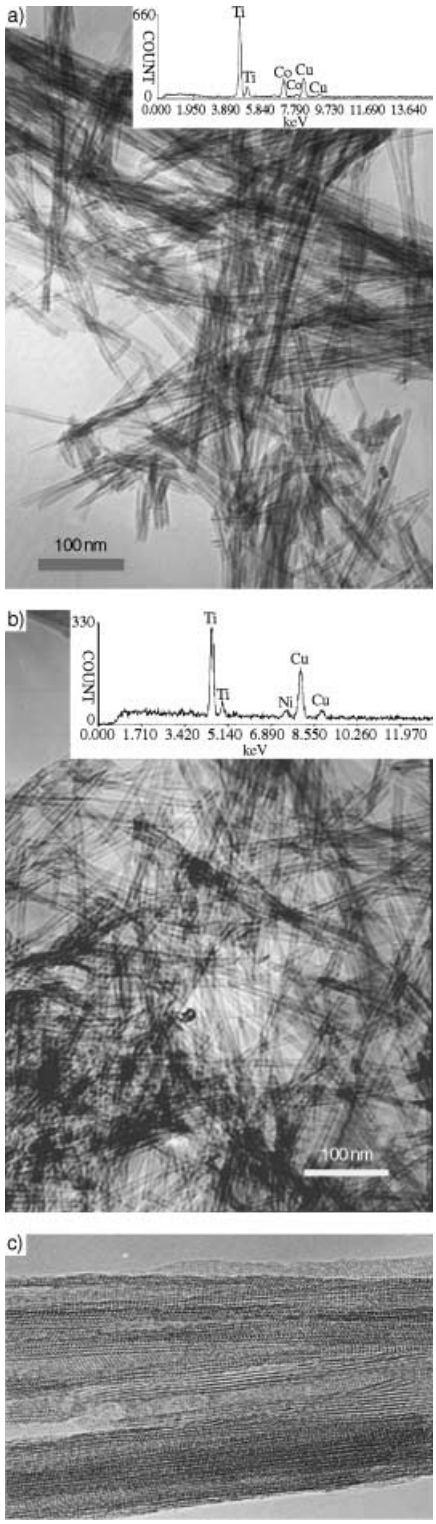

Figure 13. TEM images of a) Co-substituted nanotubes, and b) Ni-substituted nanotubes (insets show the corresponding EDXA spectrum); c) HRTEM image of Ni-substituted titanate nanotubes with layered structure.

complete. Judging from the Na-KLL peaks, the residual sodium was negligible, except for the sample substituted with Ag^+. This is reasonable to expect since hydrous titanate sheets serve as a solid-state acid in this case. The interaction between negatively charged anionic sheets and bivalent cationic ions

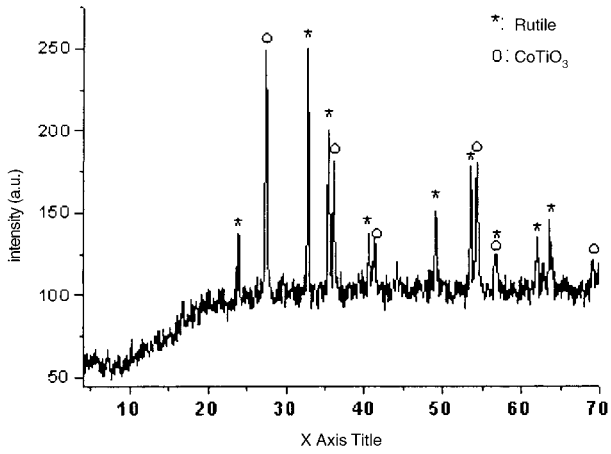

Figure 14. The XRD pattern of titanate nanotubes after thermal treatment at 850 °C, indicating the formation of $CoTiO_3$ and TiO_2 without the presence of sodium titanate.

should be larger than that with monovalent Ag^+ because of the higher effective charge density and correspondingly stronger electronic interactions. Notably, when we tried to reduce the substituted elements such as Cu^{2+} ions, which should be very easily reduced when left in a solution containing excess amounts of aqueous hydrazine,[33] we were surprised to find that no elemental copper was formed, even after tens of hours of hydrothermal treatment at 120 °C. The only explanation was that these ions were tightly bound into the lattice, and therefore prevented them from being reduced into metals.

In the substitution process, ammonium ions were also substituted into the crystal lattice. This was confirmed by TGA (Figure 15a): DTA indicated three weight loss peaks of Co-substituted nanotubes (Figure 15b) rather than the two peaks of the starting materials (Figure 15c). The first two peaks were considered to correspond to the dehydration process, and the weight loss peak positioned at 170–250 °C was considered to be caused by the loss of ammonium species.[34]

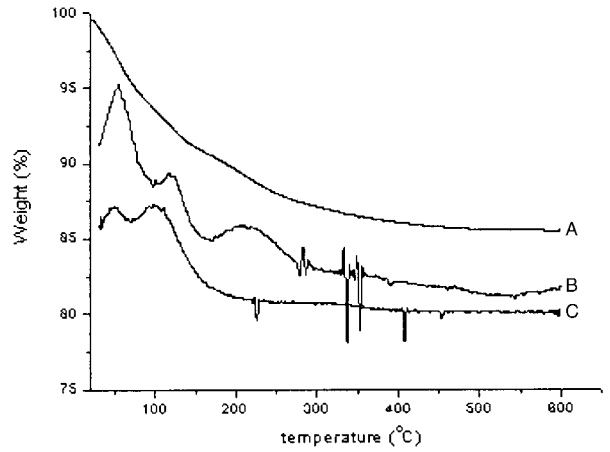

Figure 15. TGA and DTA studies on substituted and starting titanate nanotubes: a) TGA studies of titanate nanotubes substituted with Co^{2+}; b) DTA plots of the Co-substituted titanate nanotubes; c) DTA plots of the starting nanotubes, indicating two weight loss peaks.

The specific surface area could be increased by ion exchange. The BET surface area of the original (starting) nanotubes was 99 $m^2 g^{-1}$, while that of Co-substituted titanate nanotubes increased to 243 $m^2 g^{-1}$, which would be advantageous for the application of the nanotubes as catalysts.

The ion exchangeability provides an effective method to introduce functional ions. Magnetic semiconductors, which make use of spin rather than electron charges to transform reading and writing information, are highly desired and extremely attractive in the development of new multifunctional devices for optoelectronics and information storage.[35] Doping magnetic ions into host lattices to form dilute magnetic semiconductors has been realized for transition metals in titanium dioxides by using laser molecular-beam epitaxy techniques under high temperature and high vacuum.[35a] In this investigation, transition-metal ions were introduced, based on electrostatic interactions between negatively charged host lattice and positively charged cationic ions, by simply stirring the nanotubes and the ammonia solution of the corresponding ions at room temperature.

The temperature-dependent molar magnetic-susceptibility data for Co-substituted nanotubes, obtained in the temperature range 4–300 K under 5000 G on a SQUID magnetometer, is shown in Figure 16a. Calculated from the TGA (the

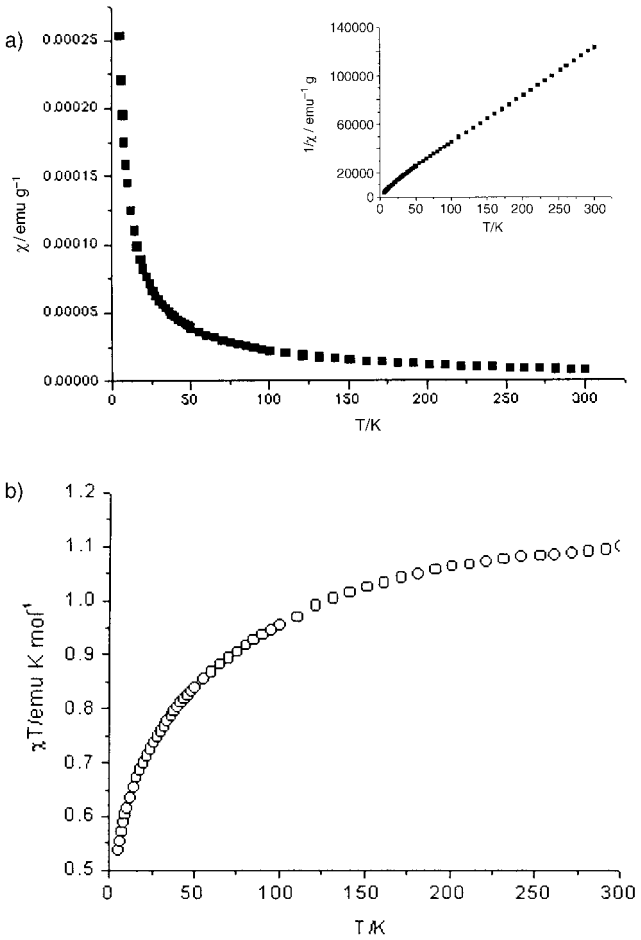

Figure 16. Magnetic susceptibility of Co-substituted nanotubes. a) χ_M and $1/\chi_M$ versus temperature T plots for Co-substituted nanotubes; b) χT versus temperature T plots for Co-NT.

molar ratio of H_2O to NH_3 was estimated to be 2.33:1.13 as calculated by the stages in mass loss) and the EDXA results (the molar ratio of Co to Ti was estimated to be 1:3.5), the approximate chemical composition was formulated as $CoO \cdot 3.5\,TiO_2 \cdot 2.33\,H_2O \cdot 1.13\,NH_3$ with a molecular weight of 422. The room temperature value of $\chi_M T$ is about 1.1 emu K mol^{-1} per Co^{2+} ion lower than the expected value (2.57 emu K mol^{-1}, $g = 2.34$) for a magnetically isolated high-spin Co^{II} ion ($S = 3/2$). With the decrease of the temperature, $\chi_M T$ decreases uniformly (Figure 16b). The magnetic susceptibilities obey the Curie–Weiss law in the temperature range 23–300 K, giving a Weiss constant of -14.3 K. This was due to the composite effects of the antiferromagnetic Co^{II}–Co^{II} interaction, the zero-field splitting of Co^{II} ions and also the orbital contribution of Co^{II} ($t_{2g}^5 e_g^2$).

Not only the magnetic properties, but also the optical properties of the titanate nanotubes were modifiable by introducing different transition-metal ions. Figure 17 shows the UV/Vis diffuse-reflectance spectra of titanate nanotubes substituted with different transition-metal ions. The band-gap energy of the starting titanate nanotubes was determined to be 3.1 eV, while the Co^{2+}-, Cu^{2+}-, and Ni^{2+}-substituted nanotubes showed a strong, broad absorption in the visible-light range due to the d–d transition of these transition-metal ions. This implied that these nanotubes might be excited by visible light by the introduction of transition-metal ions.

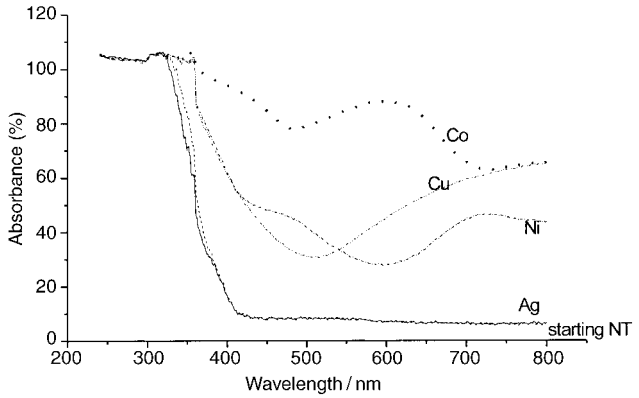

Figure 17. The UV/Vis diffuse-reflectance spectra of different titanate nanotubes (starting nanotubes (NT) and corresponding substituted elements are marked).

The nanotubes were demonstrated to be photoactive as evidenced by the photoluminescence spectra (Figure 18). Blue emission spectra around 400 nm were observed for the titanate nanotubes at room temperature with excitation at 236 nm. This behavior was noteworthy because most titanates do not show luminescence at room temperature.[27] Titanates are often used in photocatalysis[36] and solar-energy conversion.[37] The tubular structure provides an opportunity for encapsulation of visible-light excitable materials such as CdS or Fe_2O_3 into the tubes.[38] Thus, besides serving as a kind of molecular sieve for separating noble-metal ions (i.e. environmental purification), the nanotubes might find applications in photocleavage of water, photocatalysis, and even for fuel-cell electrolytes.[39]

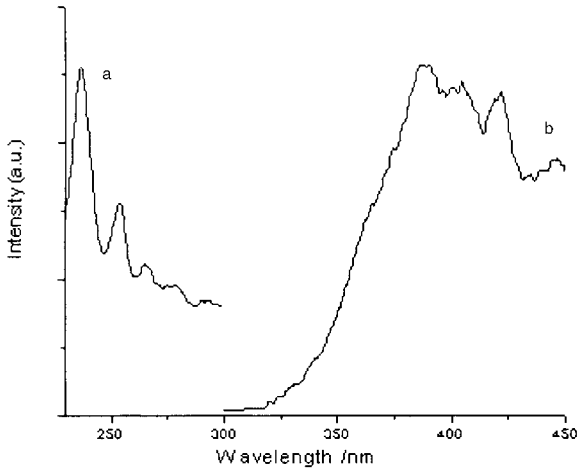

Figure 18. The photoluminescence spectra of titanate nanotubes: a) the excitation spectra of titanate nanotubes with emission at 390 nm; b) the emission spectra of titanate nanotubes with excitation at 236 nm.

Conclusion

Titanate nanotubes were synthesized by a simple hydrothermal method, followed by washing with water and dispersion with alcohol. The equipment required was simple and alkali solutions were reusable, which shows that this method has potential for use for large-scale industrial production. Ion-exchange reactions revealed that the nanotubes prepared in this way were titanate nanotubes rather than TiO_2 nanotubes. The ion exchangeability also provided the opportunity to prepare complex transition-metal oxide nanotubes, which would be ideal materials for heterogeneous catalysis or catalysts supports, as well as a candidate for host–guest chemistry, ion-exchange, and as an absorbents. The nanotubular structure yielded high specific surface areas and should be advantageous for the ion-exchange process. Optical and magnetic properties could be introduced or manipulated by introducing different kinds of cations.

Acknowledgement

We thank Dr. Z. X. Deng, Prof. R. J. Wang, Dr. H. Z. Kou, and Prof. L. M. Peng for helpful discussions. This work was supported by NSFC (20025102, 50028201, 20151001) and the state key project of fundamental research for nanomaterials and nanostructures.

[1] a) C. T. Kresge, M. E. Leonowiez, W. J. Roth, J. C. Bartuli, J. S. Beck, *Nature*, **1992**, *352*, 710–712; b) A. Corma, *Chem. Rev.*, **1997**, *97*, 2373—2419; c) A. Corma, M. Diaz-Cabanas, J. Martinez-Triguero, F. Rey, J. Rius, *Nature*, **2002**, *418*, 514–517.

[2] a) P. D. Yang, D. Y. Zhao, D. I. Margolese, B. F. Chmelka, G. D. Stuky, *Nature*, **1998**, *396*, 152–155; b) D. M. Antonelli, J. Y. Ying, *Angew. Chem.* **1995**, *107*, 2202–2206; *Angew. Chem. Int. Ed. Engl.* **1995**, *34*, 2014–2017.

[3] a) Z. T. Zhang, Y. Han, F. S. Xiao, S. L. Qiu, L. Zhu, R. W. Wang, Y. Yu, Z. Zhang, B. S. Zou, Y. Q. Wang, H. P. Sun, D. Y. Zhao, Y. Wei, *J. Am. Chem. Soc.*, **2001**, *123*, 5014–5021; b) D. T. On, S. Kaliaguine, *Angew. Chem.* **2001**, *113*, 3348—3351; *Angew. Chem. Int. Ed.* **2001**, *40*, 3248–3251; c) T. Asefa, M. J. Maclachlan, M. Coombs, G. A. Ozin, *Nature*, **1999**, *402*, 867–870.

[4] S. Iijima, *Nature* **1991**, *354*, 56 – 59.
[5] a) H. J. Dai, E. W. Wong, C. M. Liber, *Science* **1996**, *272*, 523 – 526; b) S. Frank, P. Poncharal, Z. L. Wang, W. A. Heer, *Science* **1998**, *280,* 1744 – 1746; c) S. Paulson, A. Helser, M. Nardelli, *Science* **2000**, *290*, 1742 – 1744.
[6] W. Z. Li, S. S. Xie, L. X. Qian, B. H. Chang, B. S. Zou, W. Y. Zhou, R. A. Zhao, G. Wang, *Science* **1996**, *274*, 1701 – 1703.
[7] T. W. Odam, J. L. Huang, P. Kim, C. M. Lieber, *Nature* **1998**, *391*, 62 – 64.
[8] a) G. Hummer, J. C. Rasaiah, J. P. Noworyta, *Nature* **2001**, *414*, 188 – 190; b) J. Chen, M. A. Hamon, H. Hu, Y. S. Chen, A. M. Rao, P. C. Eklund, R. C. Haddon, *Science* **1998**, *282*, 95 – 98.
[9] a) N. G. Chopra, R. J. Luyken, K. Cherry, V. H. Crespi, M. I. Cohen, S. G. Louie, A. Zettl, *Science* **1995**, *269*, 966 – 967; b) Z. Wengsieh, K. Cherrey, N. G. Chopra, X. Balse, Y. Miyamoto, A. Rubio, M. L. Cohen, S. G. Louie, A. Zettl, R. Gronsky, *Phys. Rev. B* **1995**, *51*, 11 229 – 11 232; c) O. Stephan, P. M. Ajayan, C. Colliex, P. Redich, J. M. Lambert, P. Bernier, Lefin, P. *Science* **1994**, *266*, 1683 – 1685; d) A. Zettl, *Adv. Mater.* **1996**, 8, 443 – 445.
[10] a) R. Tenne, L. Margulis, M. Genut, G. Hodes, *Nature* **1992**, *360*, 444 – 446; b) R. Tenne, *Adv. Mater.* **1995**, *7*, 965 – 968; c) Y. D. Li, X. L. Li, R. R. He, J. Zhu, Z. X. Deng, *J. Am. Chem. Soc.* **2001**, *124*, 1411 – 1415.
[11] Y. R. Hachohen, E. Grunbaum, J. Sloan, J. L. Hutchison, R. Tenne, *Nature*, **1998**, *395*, 336 – 337.
[12] M. E. Spahr, P. Bitterli, R. Nesper, M. Müller, F. Krumeich, H. U. Nissen, *Angew. Chem.* **1998**, *110,* 1339 – 1342; *Angew. Chem. Int. Ed.* **1998**, *37*, 1263 – 1265.
[13] J. A. Hollingsworth, D. M. Poojary, A. Clearfied, W. E. Buhro, *J. Am. Chem. Soc.* **2000**, *122*, 3562 – 3563.
[14] Y. D. Li, J. W. Wang, Z. X. Deng, Y. Y. Wu, X. M. Sun, D. P. Yu, P. D. Yang, *J. Am. Chem. Soc.* **2001**, *123*, 9904 – 9905.
[15] M. Côté, M. L. Cohen, D. J. Chadi, *Phys. Rev. B* **1998**, *58*, 4277 – 4280.
[16] C. N. R. Rao, B. C. Satishkumar, A. Govindaraj, *Chem. Commun.* **1997**, 1581 – 1582.
[17] P. Hoyer, *Langmuir*, **1996**, *12*, 1411 – 1413.
[18] a) T. Kasuga, M. Hiramatsu, A. Hoson, T. Sekino, K. Niihara, *Langmuir*, **1998**, *14*, 3160 – 3163; b) T. Kasuga, M. Hiramatsu, A. Hoson, T. Sekino, K. Niihara, *Adv. Mater.* **1999**, *11*, 1307 – 1311.
[19] a) C. Lettmann, H. Hinsichs, W. F. Maier, *Angrew. Chem.* **2001**, *113*, 3258 – 3262; *Angew. Chem. Int. Ed.* **2001**, *40*, 3160 – 3164; b) P. G. Smirniotis, D. A. Peña, B. S. Uphade, *Angrew. Chem.,* **2001**, *113,* 2537 – 2540; *Angew. Chem. Int. Ed.* **2001**, *40*, 2479 – 2482. c) J. C. Yu, J. G. Yu, W. K. Ho, L. Z. Zhang, *Chem. Commun.* **2001**, 1942 – 1943.
[20] a) A. Corma, P. Esteve, A. Martinez, S. Valencias, *J. Catal.* **1995**, *152*, 18 – 24; b) P. Calza, C. Pazé, E. Pelizzetti, A. Zecchina, *Chem. Commun.* **2001**, 2130 – 2131.
[21] a) Y. C. Zhu, H. L. Li, Y. R. Koltypin, Y. R. Hacohen, A. Gedanken, *Chem. Commun.* **2001**, 2616 – 2617; b) Q. H. Zhang, L. Gao, J. Sun, S. Zheng, *Chem. Lett.* **2002**, 226 – 227; c) D. S. Seo, J. K. Lee, H. Kim, *J. Crystal Growth*, **2001**, *229*, 428 – 430; d) Y. H. Zhang, A. Reller, *Chem. Commun.* **2002**, 606 – 607.
[22] a) T. Sasaki, M. Watanabe, Y. Komatsu, Y. Fujiki, *Inorg. Chem.* **1985**, *24*, 2265 – 2271; b) T. Sasaki, Y. Komatsu, Y. Fujiki, *Mater. Res. Bull.* **1987**, *22*, 1321 – 1328; c) M. Sugita, M. Tsuji, M. Abe, *Bull. Chem. Soc. Jpn.* **1990**, *63*, 1978 – 1984; d) T. Sasaki, F. Kooli, M. Iida, Y. Michiue, S. Takenouchi, Y. Yajima, F. Izumi, B. C. Chakoumakos, M. Watanabe, *Chem. Mater.* **1998**, *10,* 4123 – 4128.
[23] G. H. Du, Q. Chen, R. C. Che, Z. Y. Yuan, L. M. Peng, *Appl. Phys. Lett.* **2001**, *79*, 3702 – 3704.
[24] Y. D. Li, Synthesis and characterization of novel inorganic nanotubes and single crystal nanowires in *The third China-Sweden Meeting on Nanometer-Scale Science and Technology,* April, 22 – 25th, Beijing, China, **2001**.
[25] C. Wang, Z. X. Deng, Y. D. Li, *Inorg. Chem.* **2001**, *40*, 5210 – 5214.
[26] Q. Chen, G. H. Du, S. Zhang, L. M. Peng, *Acta Crystallogr. B* **2002**, *58*, 587 – 593.
[27] A. Kudo, T. Kondo, *J. Mater. Chem.* **1997**, *7*, 777.
[28] S. Agarwal, G. L. Sharma, R. Manchanda, *Solid State Comm.* **2001**, *119*, 681 – 686.
[29] H. M. Kim, F. Miyaji, T. Kokubo, T. Nakamura, *J. Mater. Sci. Mater. Med.* **1997**, *8*, 341 – 347.
[30] T. J. Trentler, T. E. Denler, J. F. Bertone, A. Agrawal, B. L. Colbin, *J. Am. Chem. Soc.* **1999**, *121*, 1613 – 1614.
[31] D. J. D. Corcoran, D. P. Tunstall, J. T. S. Irvine, *Solid State Ionics* **2000**, *136 – 137*, 297 – 303.
[32] a) P. D. Yang, D. Y. Zhao, D. I. Margolese, B. F. Chmelka, G. D. Stucky, *Chem. Mater.* **1999**, *11*, 2813 – 2826; b) D. M. Antonelli, J. Y. Ying, *Angew. Chem.* **1996**, *108,* 461 – 464; *Angew. Chem. Int. Ed. Engl.* **1996**, *35*, 426 – 430; b) J. S. Chang, S. E. Park, Q. M. Gao, G. Férey, A. K. Cheetham, *Chem. Commun.* **2001**, 859 – 860.
[33] a) Y. J. Dong, Y. D. Li, C. Wang, A. L. Cui, Z. X. Deng, *J. Colloid. Interf. Sci.* **2001**, *243,* 85 – 89; b) H. G. Zheng, Y. D. Li, C. W. Li, H. Z. Zhao, Y. H. Lin, Y. T. Qian, *Acta Phys.-Chim. Sin.* **1997**, *13*, 974 – 977.
[34] H. S. Potdar, S. B. Deshpande, A. S. Deshpande, Y. B. Khollam, A. J. Patil, S. D. Pradhan, S. K. Date, *Int. Inorg. Mater.* **2001**, *3*, 613 – 623.
[35] a) Y. Matsumoto, M. Murakami, T. Shono, T. Hasegawa, T. Fukumura, M. Kawasaki, P. Ahmet, T. Chikyow, S. Koshihara, H. Koinuma, *Science* **2001**, *291*, 854 – 856; b) H. R. Heulings, X. Y. Huang, J. Li, T. Yuen, C. L. Lin, *NanoLett.* **2001**, *1*, 521 – 525.
[36] Y. Matsumoto, M. Murakami, T. Shono, T. Hasegawa, T. Fukumura, M. Kawasaki, P. Ahmet, T. Chikyow, S. Koshihara, H. Koinuma, *Science* **2001**, *291*, 854 – 856.
[37] a) S. Ychida, Y. Yamamoto, Y. Fujishiro, A. Watanabe, I. Osamu, T. Sato, *J. Chem. Soc. Faraday Trans.* **1997**, *93*, 3229 – 3234; b) M. Yanagisawa, S. Ychida, T. Sato, *Int. J. Inorg. Mater.* **2000**, *2*, 339 – 346; c) J. H. Choy, H. C. Lee, H. Jung, S. J. Huang, *J. Mater. Chem.* **2001**, *11*, 2232 – 2234.
[38] a) T. Sato, Y. Yamamoto, Y. Fujishiro, S. Uchida, *J. Chem. Soc. Faraday Trans.* **1996**, *92*, 5089 – 5092; b) T. Sato, K. Masaki, K. Sato, Y. Fujishiro, A. Okuwaki, *J. Chem. Technol. Biotechnol.* **1996**, *67*, 339 – 344.
[39] a) A. Kudo, E. Kaneko, *Micro. Meso. Mater.* **1998**, *21*, 615 – 620; b) D. J. D. Corcoran, D. P. Tunstall, J. T. S. Irvine, *Solid State Ionics* **2000**, *136 – 137*, 297 – 303.

Received: October 8, 2002
Revised: December 11, 2002 [F4394]